



Article

Effects of Ion Cyclotron Frequencies on Human Resistance and Reactance in 31 Healthy Subjects

Aldo Liguori ¹, Larissa Brizhik ² , Stefano Liguori ³, Laura Silli ³, Sergio Bangrazi ¹, Filomena Petti ¹, Medardo Pinti ¹, Maria Ilaria Pistelli ⁴ , and Livio Giuliani ^{5,6,*}

¹ School of Acupuncture, Paracelso Institute, 00153 Rome, Italy

² Bogolyubov Institute for Theoretical Physics, The National Academy of Sciences of Ukraine, 03143 Kyiv, Ukraine

³ Clinic Center, Paracelso Institute, 00153 Rome, Italy

⁴ RINA Consulting—Center of Materials Development, 00128 Rome, Italy

⁵ International Commission for Electromagnetic Safety (ICEMS), 30171 Venice, Italy

⁶ European Cancer and Environment Research (ECERI), 1000 Bruxelles, Belgium

* Correspondence: giuliani.livio@gmail.com

Simple Summary: Acupuncture meridians and points are not physiologically detectable as an organic tissue. Brizhik et al. (2009) suggested they are thin hydric channels, sailed by solitons, able to carry information between remote sites of our organism. In the case, the main role of needles should be to replace a channel break thanks to a conductive metal bridge. Such role of meridians should be enhanced in acupoints. There should be detected an enhanced conductivity with respect to around tissue. The aim is to test clinically such enhanced conductivity and to verify that it can be induced also by electromagnetic fields, that can be complementary to needles.



Citation: Liguori, A.; Brizhik, L.; Liguori, S.; Silli, L.; Bangrazi, S.; Petti, F.; Pinti, M.; Pistelli, M.I.; Giuliani, L. Effects of Ion Cyclotron Frequencies on Human Resistance and Reactance in 31 Healthy Subjects. *Radiation* **2022**, *2*, 357–375. <https://doi.org/10.3390/radiation2040027>

Academic Editor: Gabriele Multhoff

Received: 16 August 2022

Accepted: 17 October 2022

Published: 26 October 2022

Publisher's Note: MDPI stays neutral with regard to jurisdictional claims in published maps and institutional affiliations.

Abstract: In order to test the theory of Brizhik et al. about the dynamic allocation of acupuncture meridians on human body and their role as hydric paths for solitons, we tested the effect of both acupuncture and exposure to extremely low frequencies (ELF) tuned with suitable ion cyclotron frequencies. The similarity of the effects, inducing variations of body impedance measured in well-known acupuncture points, up to the interchangeability and the synergy of the two treatments, the mechanic and the electromagnetic ones, turns to be evidence of the validity of the theory. Resistance and reactance variations have been detected in a group of 31 healthy volunteers before and after stimulation with a standard sequence of cyclotron frequencies, emitted from an innovative electromagnetic therapy (EMT) device. These variations were then compared with the variations produced by the well-known percutaneous stimuli of mechanical and piezoelectric nature, and, in particular in this work, acupuncture. Our results show that the observed variations can be considered as significant in both groups: cyclotron and acupuncture. The greater variations brought about by the cyclotron treatment stand out clearly.

Keywords: acupuncture; meridian; emitted electromagnetic therapy; geomagnetic field; ion cyclotron resonance; Schumann frequencies; water conductivity; bio-impedance; bio-resistance



Copyright: © 2022 by the authors. Licensee MDPI, Basel, Switzerland. This article is an open access article distributed under the terms and conditions of the Creative Commons Attribution (CC BY) license (<https://creativecommons.org/licenses/by/4.0/>).

1. Introduction

1.1. Origin of the Dynamical Allocation of Acupuncture Points

The basic notion of Eastern Medicine and experimental evidence of Western Complementary Medicine are acupuncture points, which in the Western medical literature are often called ‘biologically active points’. Their dissemination in the body appears as a lattice whose branches are named meridians, connected by nodes: the acupuncture points. Acupuncture points and meridians do not have a stable morphological structure and their location undergoes variations, although of a small entity. From a practical point of view,

this kind of delocalization is not a serious problem, since practitioners are able to recognize the lattice despite its variability. Moreover, this finite variability of the acupuncture points positions indicates that they are dynamic entities formed in the self-organization of living matter, which depends on its metabolism and physiological conditions, among other factors. Such variability are inconvenient from the point of view of Western Medicine, since physiology is used to examine the subject of its studies as a solid matter-made subject, and therefore, stable. Nevertheless, there is experimental evidence that acupuncture points have distinctive electrical and optical properties [1]; In particular, their electrical conductivity differs from that of surrounding tissues [2–4], and their refractive indices are also different. It has been suggested that meridians are “flows of matter, energy, and information, which can be not uniformly spread over the organism due to self-trapping induced by the correlated coherent domains of interfacial water” [5]. In this frame, the disposal of interfacial water “forms the dynamical pathways as wave-guides, along which these flows can take place via soliton mechanisms”. Thus, we can argue that meridians are a sort of continuous “channels” in the body, interconnected by acupuncture points as nodes whose formation is allocated dynamically, depending on the disposal of interfacial water and other physiological conditions (there are experimental evidences that the positions of the relevant acupuncture points change during or after treatment [6]. In other words, one of the physical interpretations of the meridians, as well as their nodes, originate from the spread of interfacial water: a water with a high presence of coherent domains, i.e., clusters of water molecules whose quantum oscillations are tuned with the oscillations of the inner trapped electromagnetic field [7]. Coherent water drives solitons, carriers of information and energy, through the body, which can be stimulated either by endogenous electromagnetic fields, originating from electric currents that are typical for each tissue, or by exogenous stimuli.

The latter are not only electromagnetic stimuli, although every stimulus is able to provide energy to coherent domains, which act as reservoirs of energy captured from the environment and are able to return energy in a unique degree of freedom, i.e., the electromagnetic one, to ion currents needed to perform every electrochemical reaction in living tissues.

While we can recognize that the delocalization of meridians and their nodes is a consequence of the liquid state of water, we can also recognize that the variability of the localization of acupuncture nodes is tight, since endogenous electromagnetic fields, able to stimulate solitons are originated by cells. Their frequency, amplitude, and waveform are typical for each tissue [8,9]. Thus, solitons are forced to follow a unique itinerary, which, even seemingly randomized, is traced by the sequence of tissues underlying derma. This itinerary is the sequence of the pathways as the waveguides of the energy and information flow are formed as a result of the nonlinear processes similar to electromagnetic field self-focusing in the nonlinear optical medium and as the nonlinear entities are dynamically stable.

1.2. Higher Conductivity in Acupuncture Points

There is another point that must be explained. Why, in acupuncture points, is the electrical conductivity higher than in the surrounding tissues? In the reasonable hypothesis that such an electrical property of acupuncture points is aroused by electromagnetic fields, what is their origin? We argue that the biological environment is the origin of such electromagnetic fields, but they do not belong to the class of exogenous stimuli that recharge coherent domains of interfacial water forming meridians or their nodes. These electromagnetic fields, rather, allow the increase of conductivity of the incoherent fraction of interfacial water, forming meridians or accumulating ions in their nodes, and in such a way, favoring the propagation of solitons. It has been shown that magnetic fields at cyclotron frequency of hydronium ion H_3O^+ and of its hydrates are able to increase the conductivity of water [10]. Even the optical properties of water, the refraction index included, are altered [11], which indicates the self-consistent nature of meridians and the formation of their nodes. As a

matter of fact, the main peaks of Schumann frequencies match the ion cyclotron frequency of Zundel Cation H_5O_2^+ or other hydrates of hydronium, where the geomagnetic field is about 40 μT and the magnetic inclination is about 60° , as in Middle Italy. In other countries, the geomagnetic strength increases with the latitude while magnetic inclination decreases. Moreover, Schumann frequencies vary. Therefore, we can argue that electrical conductivity of acupuncture points can vary depending on the intensity of Schumann frequencies, which are an environmental factor, and thus, highly variable: more intense when a thunderstorm is near us, weaker when far.

Therefore, we shall consider physical properties of meridians and their nodes, both optical and electrical, randomized as randomized is their location on the body, though approximately and dynamically stable.

2. Materials and Methods

2.1. Aim

The aim of this work is to verify the variations of resistance and reactance detected in a group of healthy volunteers before and after stimulation with a standard sequence of cyclotron frequencies, emitted by an innovative electromagnetic therapy (EMT) device. These variations were then compared with the variations produced by the well-known percutaneous stimuli of a mechanical and piezoelectric nature, such as those of acupuncture, well documented in the literature [12,13].

Eventually, under the hypotheses reported in Section 1, we expect that both electromagnetic and acupuncture treatments improve the conductivity and increase the ratio phase angle of impedance in acupuncture points.

In more general terms, the aim is to harvest clinical data highlighting the role of exogenous magnetic fields in human health, in the frame of the previous achievements [14].

2.2. Design

Stimulations and clinical observations were performed from 3 September 2018 until 30 April 2019. Volunteers underwent two sessions, one of abdominal acupuncture and one of exposure to EMT, generating a magnetic field at cyclotron frequencies. The sessions were taken in two different days at an interval of one week, starting either with abdominal acupuncture or with EMT cyclotron frequencies, in intentionally random mode.

The EMT device has been set to emit the following frequencies in succession, for a duration of 15 min each: 1.89 Hz, 7.88 Hz, 30.66 Hz, 50.56 Hz, and 15.72 Hz. Resistance, reactance, phase angle, normalized resistance, and normalized reactance at different time moments, i.e., T0, T1, and T2, were detected with BYODINAMICS, where T0 is before treatment, T1 is immediately after treatment, and T2 is 8 h after the end of the treatment.

2.3. Inclusion/Exclusion Criteria

The sample included 35 healthy volunteers, of normal weight, both genders, ageing 30 to 65, not currently subject to any kind of therapy (antihypertensive therapy, antidiabetic therapy, hormonal therapy, etc.). The volunteers were chosen after urine analysis and standard blood test (CBC and electrolytes, ESR, CRP, glycated HB, glycemia, uricemia, γ GT, protein electrophoresis, TSH, FT3, FT4, creatinine, and BUN), in order to exclude any evidence of one or more of the most frequent metabolic and thyroid diseases, and upon informed written consent [15]. Volunteers that showed even only one blood chemistry value outside usual laboratory standards were excluded. Eventually 31 volunteers were accepted for the trial, as in Table 1.

Table 1. Healthy volunteers' data (sex, age, weight, height).

	M/F	Age (y)	Weight (Kg)	Height (cm)
(1)	M	38	70	170
(2)	M	20	60	175
(3)	F	15	51	174
(4)	F	53	64	168
(5)	F	50	61	178
(6)	F	51	63	175
(7)	F	52	53	180
(8)	M	51	76	178
(9)	M	50	66	165
(10)	F	52	68	168
(11)	F	19	53	161
(12)	F	53	62	174
(13)	M	51	61	176
(14)	M	17	53	172
(15)	M	16	51	178
(16)	F	53	58	174
(17)	F	52	63	172
(18)	F	17	54	176
(19)	F	51	70	174
(20)	M	49	69	168
(21)	F	51	81	172
(22)	M	49	62	174
(23)	F	52	57	172
(24)	F	19	55	171
(25)	F	52	64	170
(26)	M	19	53	167
(27)	F	14	49	170
(28)	F	17	54	168
(29)	M	17	55	169
(30)	F	16	49	155
(31)	F	13	48	160
average	0.355 *	36.42 ± 3.226	59.77 ± 2.839	171.09 ± 1.290
std. dev.	* M/F ratio	17.67	±15.55	±7.07

* M/F ratio is the ratio of Male to Female patients.

2.4. Instructions before and after Sessions

Volunteers were recommended to arrive in the morning with an empty stomach. They were required to urinate and empty their bladders immediately before treatment as well as to drink 0.2 L of water right after urination. After treatment, they were asked to have a light breakfast, free of sugar, jam, honey, and fruit, and a lunch limited to 150 g of meat. They were also instructed to limit physical movement during the day and to reduce their usual work and/or occupations to a minimum, since physical efforts and heavy meals are supposed to alter the impedance indices.

2.5. Resistance and Reactance Measurements: Byodinamics Device and Its Use with Probes

BYODINAMICS is an impedance analyzer (providing resistance and reactance), through direct measurements on the body surface. It is usually used for an analysis of body composition such as fat mass, lean mass, and intra- and extracellular body water. The test was made by using self-adhesive patch electrodes. Two rectangle-shaped patch electrodes, sized $(23 \times 34) \text{ mm}^2$, were placed transversely on the back of the right hand, the first one between half the length of the metacarpals on the back of the right hand and the 4th and 5th metacarpophalangeal joints, transversely to the $5-4^\circ$ and $4-3^\circ$ metacarpal interspaces, and the second one at the level of the wrist 5 cm away from the first electrode. Likewise, two other electrodes of equal shape and size were placed transversely on the back of the right foot, one proximal to the metatarsal-phalangeal joint, transversely to the $5-4^\circ$ and $4-3^\circ$ metatarsal interspaces, and the other one near the ankle 5 cm away from the first patch.

The main parameters detected in this test are the following:

- Resistance (R_z, Ω): resistance is a bioelectric parameter in inverse proportion to the amount of extracellular body fluid present in the body: the more water, the lower the resistance [16–18].
- Reactance (X_c, Ω): reactance is a bioelectrical parameter in direct proportion to the density of cells in the tissues: with equal body fluids, the more reactance, the more cells or intracellular water [19,20].
- Phase angle ($X_c/R_z \times 180/\pi$): the phase angle is a linear method to measure the ratio between reactance (X_c) and resistance (R_z) detected by the current bioimpedance analysis and is a numerical value that expresses the ratio between intra- and extracellular water volumes [21–24]. The impedance measurements and the EMT and abdominal acupuncture sessions were carried out in a room at a constant temperature of 26°C .

2.6. Ion Cyclotron Resonance Frequency

Ion Cyclotron Resonance (ICR) is a phenomenon associated with the movement of ions, which form a circular motion pass to a spiral movement when subjected to a cyclotron-tuned magnetic field (with amplitude in the same order as the one present on the Earth surface).

In the present experiment, the cyclotron frequency f was calculated according to the formula:

$$f = B_{0//}q/(2\pi m) \quad (1)$$

where q and m are, respectively, the charge and the mass of the involved ion and $B_{0//}$ is the component of the geomagnetic induction B_0 , parallel to the Earth surface, i.e., $B_{0//} = B_0 \cos I_0$, where I_0 is the geomagnetic inclination.

2.7. The MED CRI Device for Electromagnetic Cyclotron Treatment: Exposure System to Magnetostatic and Alternated Magnetic Fields

This study adopts an innovative EMT device, capable of being adjusted to emit surface electromagnetic waves at frequencies up to 24 Megahertz. The output power from the generator is 20–25 W. The magnetic induction of the emitters is 3 to 15 μT .

This innovative apparatus has been equipped with special devices in order to avoid geomagnetic interference in the treatment area. These devices are capable of zeroing the vertical component (z) of the Earth magnetic field. The alignment of the device to the south–north direction allows to maximize the superficial geomagnetic flux (Figure 1).

In the adopted procedure, the values of the three components of the geomagnetic field (x, y, z) in the bed zone of treatment were checked with suitable probes before starting each session of therapy.

To eliminate the interference given by the Earth magnetic field, the bed was aligned in a position where the value of the Earth magnetic component y (at EST) was equal to

zero. In order to zero the vector component z , a pair of vertical axis Helmholtz coils was powered up to create a magnetic flux in the direction opposite to that of z .



Figure 1. MED CRI device for cyclotron electromagnetic treatment. The value of the vector component south–north of the geomagnetic field, parallel to the powered alternating magnetic field, was increased by creating a stronger static magnetic field ($40 \mu\text{T}$), in the same direction of the alternating field. The selected ion cyclotron frequencies for tests were computed as in Equation (1).

These two emitters, both of suitable dimensions, have been placed above and below the bed, in a horizontal position and parallel to each other. The three vertical coils provide the alternating magnetic field parallel to the superficial Earth magnetic field, artificially produced.

2.8. Selection of Frequencies and Timing of Administration

The MED CRI device has been set to emit the following frequencies in succession, for a duration of 15 min each:

- Estimated resonance frequency of the water coherent domains: 1.89 (1.87) Hz;
- Schumann main peak frequency (ion resonance frequency of hydroxonium tetrahydrate): 7.88 (7.83) Hz;
- Resonant frequency of the divalent calcium ion: 30.66 (30.44) Hz;
- Resonant frequency of the divalent magnesium ion: 50.56 (50.19) Hz;
- Resonant frequency of the monovalent potassium ion: 15.72 (15.60) Hz.

Numbers in brackets are the nominal cyclotron frequencies of the corresponding cations, which in the experiment were increased by 0.7% to take into account the quasi-static field self-induced by the ionic currents aroused in the cells of the organism under exposure.

The frequencies range between 1.87 Hz and 50.56 Hz; altogether, the selected frequencies require a treatment time of 1 h and 15 min for each session.

The ion resonance frequency of the coherence domains was selected in view of the formation of the mixed coherence domains, a prerequisite of the Liboff-Zhadin effect releasing the required energy for the ionic currents [25,26], promoters of the cellular and enzymatic

metabolism, which was the goal of the present research. The Schumann frequency was selected to enhance water conductivity through the ion cyclotron resonance of the eigen cation (hydronium tetramer) [17]. The Ca and K ion cyclotron frequencies were selected to enhance the calcium and potassium ion pumps [27,28].

2.9. Abdominal Acupuncture

Abdominal acupuncture, namely one of the microsystems of traditional Chinese acupuncture, is a technique that allows standardization of the acupuncture treatment and has an effect on the main functional components of the human body (rebalancing cenesthesia and the functions of internal organs). The selected acupoints were CV12 and CV10, located on the anterior midline between the sternum ensiform apophysis and the navel; CV6 and CV4, located on the anterior midline between the navel and the pubis; and St25 and Sp15, located on both sides of the navel. The disposable needles were selected with a diameter of 0.22 mm and a length of either 40 mm or 50 mm, according to the body build of the subject. The needles were retained for 20 min. This treatment method does not involve any kind of manipulation of the needle, which makes treatment homogeneous.

2.10. Data Detection

Resistance, reactance, phase angle, normalized resistance, and normalized reactance at different time moments, i.e., T0, T1, and T2, were detected with BYODINAMICS, where T0 is before treatment, after emptying the bladder and taking 0.2 L of water, T1 is immediately after treatment, and T2 is 8 h after the end of the treatment.

2.11. Statistical Surveys

Average, SD, and 95% confidence intervals (CI) of the parameters relative to the resistance, reactance, and phase angle were calculated at T0, T1, and T2. The Student's T test on the average values was processed to give just an approximate indication, due to the limited number of subjects submitted to analysis.

2.12. Ethics Committee

The design, study methods, and the research informed consent form were reviewed by the Ethics Committee of the Interuniversity Commission for Research on Acupuncture, an organism composed of University Professors established by AIAM (Italian Association of Acupuncture-Moxibustion and Traditional Chinese Medicine) and its approval data is 20 July 2018.

3. Protocol

In total, 56 of the initial 91 volunteers willing to participate in the study were excluded, either because their standard blood tests showed altered values or because they occasionally resorted to one or more drug therapies. Out of the 35 remaining subjects, another 4 were further excluded, 3 for health problems and 1 that moved to another city for family needs; for these reasons, they were unable to go through the second treatment cycle. Therefore, 31 subjects completed the two planned treatments at an interval of one week.

At inclusion, one month before the trial, the 31 subjects, 20 females and 11 males, had an average age of 54.32 ± 5.40 , mean weight of 65 ± 7.62 kg, and mean height of 172.10 ± 4.56 cm.

The calculation of the average values of resistance, reactance, and phase angle and the relative variations at T0, T1, and T2 showed results that can be considered as significant. The changes of the average values both in the case of cyclotron treatment and in the case of acupuncture treatment are shown in the respective diagrams (Figures 2–10).

In the diagrams, showing the variation of the average phase angle (reactance/resistance $\times 180/3.14$, a parameter that represents the ratio between intra- and extracellular water volumes), the greater variation brought about by the cyclotron treatment stands out clearly (Figures 4 and 7, and especially Figure 10).

In addition to the graphic expression of the average values of the three electromagnetic parameters, the observed variations were statistically processed. The T test was applied for purely indicative purposes, being aware that, due to the limited size of the sample and the characteristics of the sample curves, this value is not specific. The T test is reported under each diagram.

4. Results

4.1. Cyclotron

4.1.1. About Resistance

For the cyclotron frequencies group, the average resistance (Ω) is:

- 575.48 at T0;
- 580.03 at T1;
- 562.29 at T2.

A clear decrease in resistance is detectable between T0 and T2. These data encourage further research, based on larger numerical samples.

The T test shows no significant increase between T0 and T1, $p > 0.05$ ($p = 0.15$), while it is significant between T0 and T2, $p < 0.05$ ($p = 0.0038$) (Figure 2).

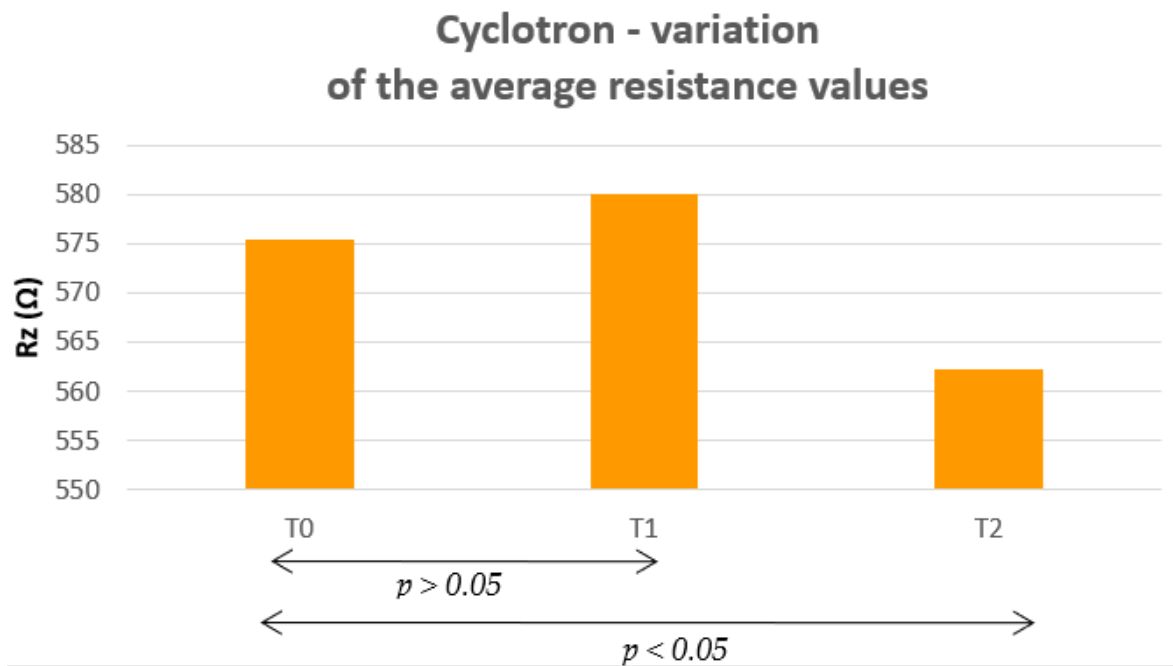


Figure 2. After exposure to ion-cyclotron emission, average resistance statistically significantly decreases at T2 in selected acupuncture points.

Table 2 shows the lower and upper values of the resistance for the 95% confidence interval and the deltas (not SD) of the averages recorded between T0 and T1 and T0 and T2.

Table 2. Cyclotron—lower and upper values of resistance (Ω). The delta of average resistance values (Ω) is included.

Resistance at:	95% Confidence Interval for the Difference		Δ_{T0}
	Lower	Upper	
T0	557	590	
T1	560	594	+4.6
T2	554	586	−13.2

4.1.2. About Reactance

For the cyclotron frequencies group, the average reactance (Ω) is:

- 51.03 at T0
- 53.77 at T1
- 54.32 at T2

The increase of reactance between T0 and T2 is clearly detectable.

The T test shows a significant increase between T0 and T1, $p < 0.05$ ($p = 0.005$), and between T0 and T2 $p < 0.001$ ($p < 10^{-8}$) (Figure 3).

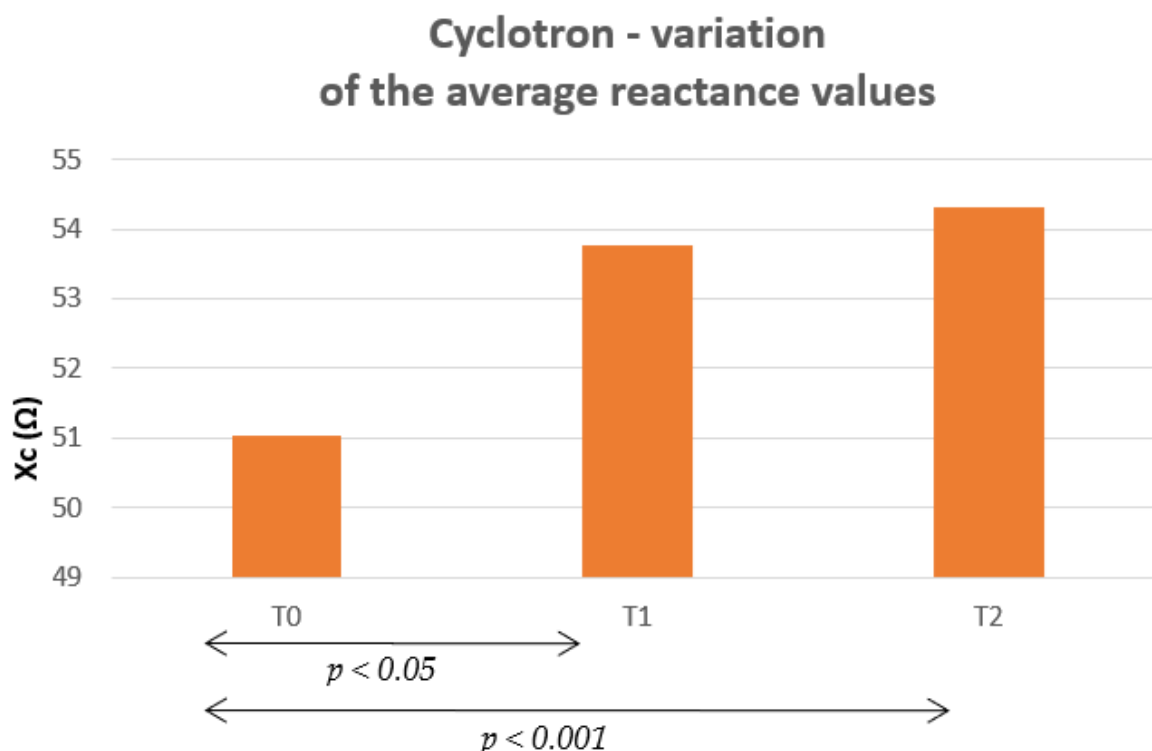


Figure 3. After exposure to ion-cyclotron emission, average reactance statistically significantly increases at T1 and further at T2, in selected acupuncture points.

Table 3 shows the lower and upper values of reactance for the 95% confidence interval and the deltas (not SD) of the averages recorded between T0 and T1, and T0 and T2:

Table 3. Cyclotron—lower and upper values of reactance (Ω). The delta of the average reactance values (Δ_{T0}) are included.

Reactance at:	95% Confidence Interval for the Difference		Δ_{T0}
	Lower	Upper	
T0	50	55	
T1	52	57	+2.7
T2	51	56	+3.3

4.1.3. About the Phase Angle

Cyclotron frequencies group, the average phase angle ($X_c/R_z \times 180/\pi$) is:

- 5.15 at T0;
- 5.24 at T1;
- 5.56 at T2.

The increase of the phase angle between T0 and T2 is clearly detectable.

The T test shows a not significant variation between T0 and T1, $p > 0.05$ ($p = 0.22$), and a very significant variation between T0 and T2, $p < 0.001$ ($p < 10^{-7}$) (Figure 4).

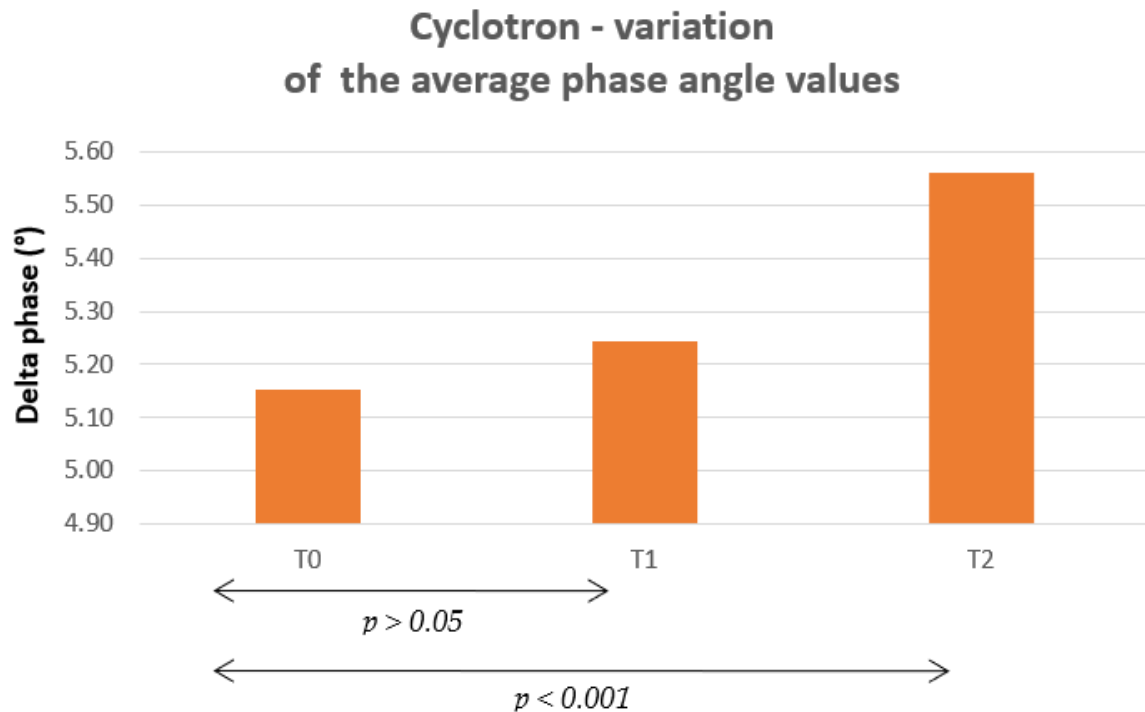


Figure 4. After exposure to ion-cyclotron emission, average phase angle statistically significantly increases at T2, in selected acupuncture points.

Table 4 shows the lower and upper values of phase angle for the 95% confidence interval and the difference (not SD) of the average values recorded between T0 and T1 and between T0 and T2.

Table 4. Cyclotron—lower and upper values of phase angle ($X_c/R_z \times 180/\pi$). The delta of the average phase angle values (°) are included.

Phase Angle (°) at:	95% Confidence Interval for the Difference		Δ_{T0}
	Lower	Upper	
T0	4.99	5.61	
T1	5.14	5.70	0.1
T2	5.12	5.67	0.4

4.2. Acupuncture

4.2.1. About Resistance

For the abdominal acupuncture group, the average resistance (Ω) is:

- 572.55 at T0;
- 576.13 at T1;
- 570.35 at T2.

A clear decrease in resistance is observable between T0 and T2. These data encourage further research based on larger numerical samples.

The T test shows a significant variation between T0 and T1, $p < 0.001$ ($p = 0.0004$). The variation is significant also between T0 and T2, $p < 0.05$ ($p = 0.047$) (Figure 5).

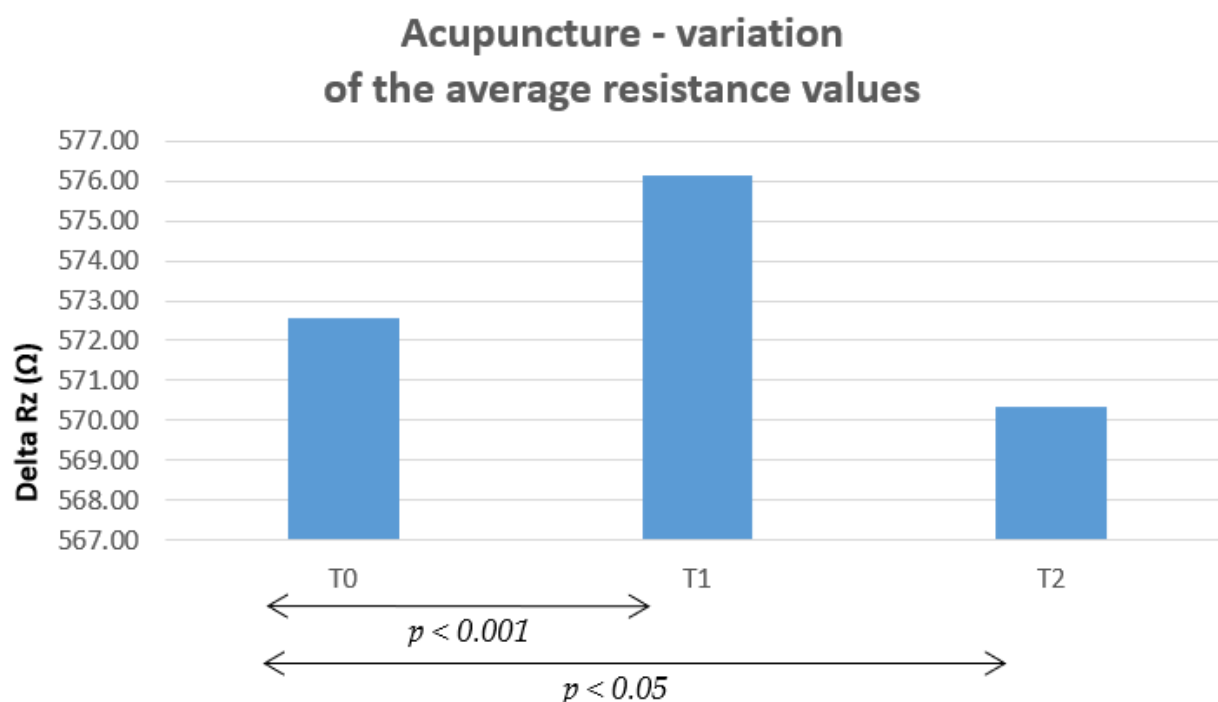


Figure 5. After acupuncture, averaged resistance increases at T1 and decreases at T2 with respect to T0 and T1, in the same selected points (both variations are statistically significant).

Table 5 shows the lower and upper values of the resistance for a 95% confidence interval and the deltas (not SD) of the averages recorded between T0 and T1 and T0 and T2.

Table 5. Acupuncture—lower and upper values of resistance (Ω). The deltas of the average resistance values (Δ_{T0}) are included.

Resistance at:	95% Confidence Interval for the Difference		Δ_{T0}
	Lower	Upper	
T0	555	590	
T1	558	594	+3.6
T2	552	589	−2.2

4.2.2. About Reactance

Abdominal acupuncture group, the average reactance (Ω) is:

- 52.55 at T0;
- 54.19 at T1;
- 53.39 at T2.

The increase of reactance between T0 and T2 is clearly visible.

The T test shows a significant increase between T0 and T1, $p < 0.05$ ($p = 0.011$), and between T0 and T2, $p < 0.05$ ($p = 0.045$) (Figure 6).

Table 6 shows the lower and upper values of reactance for the 95% confidence interval and the deltas (not SD) of the averages recorded between T0 and T1, and T0 and T2.

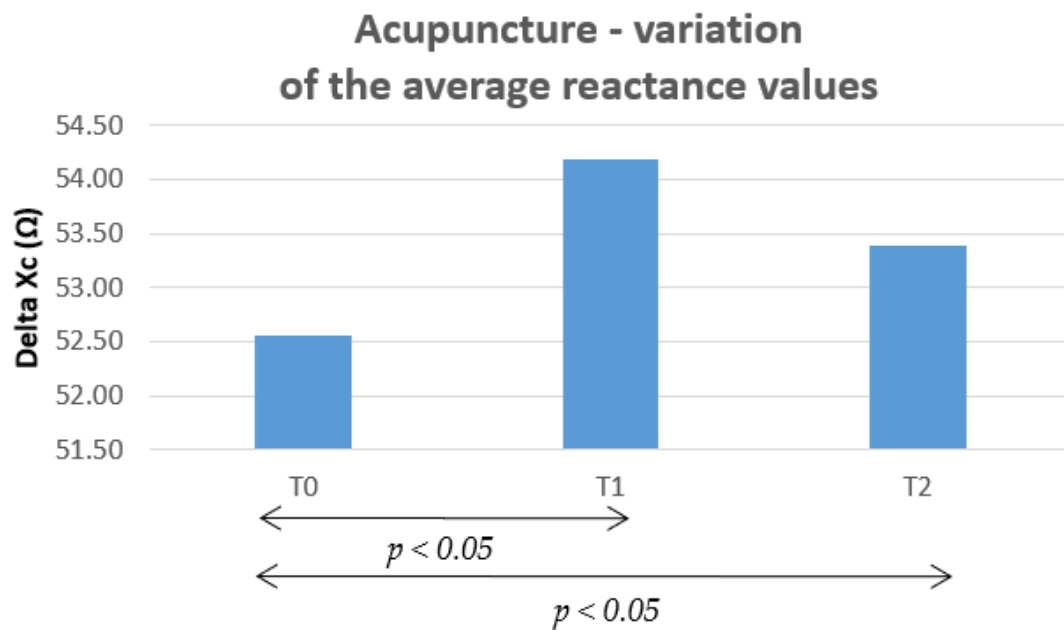


Figure 6. After acupuncture, average reactance increases more at T1 and less at T2, in the same selected points (both variations are statistically significant).

Table 6. Acupuncture—lower and upper values of reactance (Ω). The deltas of the average reactance values (Δ_{T0}) are included.

Reactance at:	95% Confidence Interval for the Difference		Δ_{T0}
	Lower	Upper	
T0	50	55	
T1	51	57	+1.7
T2	51	56	+0.8

4.2.3. About the Phase Angle

Abdominal acupuncture group, the average phase angle ($^{\circ}$) is:

- 5.29 at T0;
- 5.41 at T1;
- 5.39 at T2.

The increase of the phase angle between T0 and T2 is clearly visible.

The T test shows a significant variation between T0 and T1, $p < 0.05$ ($p = 0.038$) and a significant variation also between T0 and T2, $p < 0.05$ ($p = 0.02$) (Figure 7).

Table 7 shows the lower and upper values of the phase angle for a 95% confidence interval and the difference (not SD) of the average values recorded between T0 and T1 and between T0 and T2.

Table 7. Acupuncture—lower and upper values of the phase angle ($X_c/R_z \times 180/\pi$). The deltas of the average phase angle values ($^{\circ}$) are included.

Phase Angle at:	95% Confidence Interval for the Difference		Δ_{T0}
	Lower	Upper	
T0	4.97	5.61	
T1	5.13	5.70	+0.1
T2	5.10	5.67	+0.1

- 5.29 at T0;
- 5.41 at T1;
- 5.39 at T2.

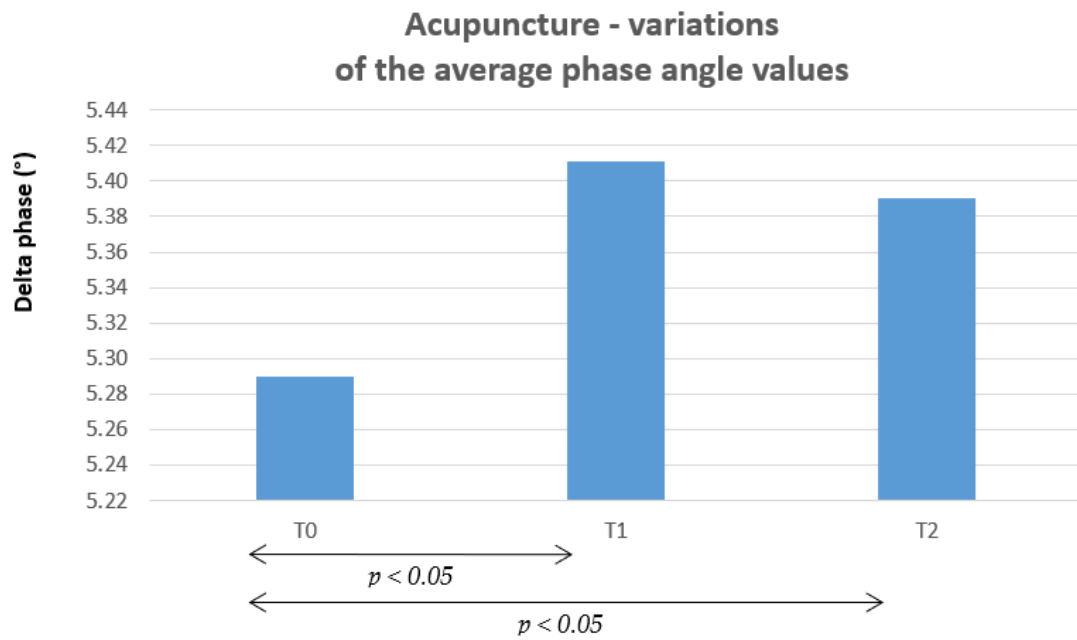


Figure 7. After acupuncture, average phase angle increases more at T1 and less at T2, in the same selected points (both variations are statistically significant). For the abdominal acupuncture group, the average phase angle is $(X_c/R_z \times 180/\pi)$.

The increase of the phase angle between T0 and T2 is clearly visible.

The T test shows a significant variation between T0 and T1, $p < 0.05$ ($p = 0.038$) and a significant variation also between T0 and T2, $p < 0.05$ ($p = 0.02$) (Figure 7)

4.3. Cyclotron vs. Acupuncture

Figures 8–10 compare the variations of the resistance, reactance, and phase angle in the cyclotron group vs. the acupuncture group.

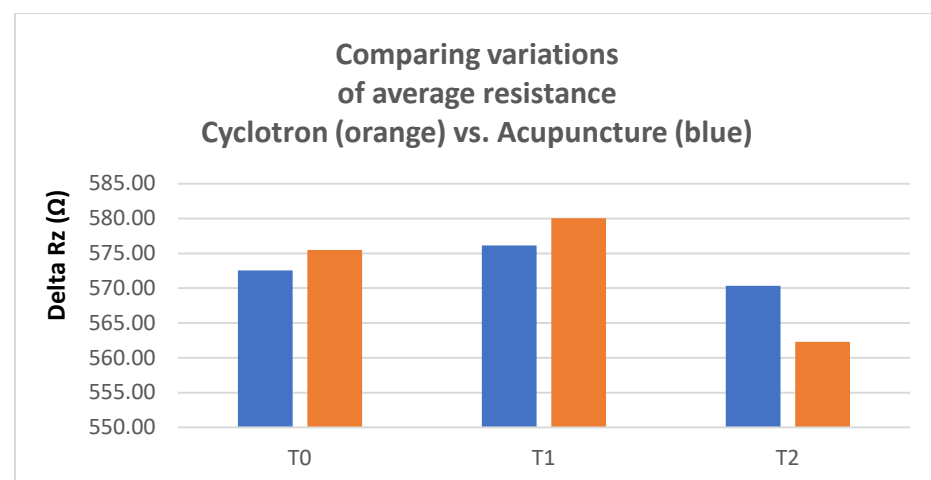


Figure 8. Trends of the average resistance are the same after acupuncture and after exposures to ion cyclotron emission, compared at the same acupuncture points.

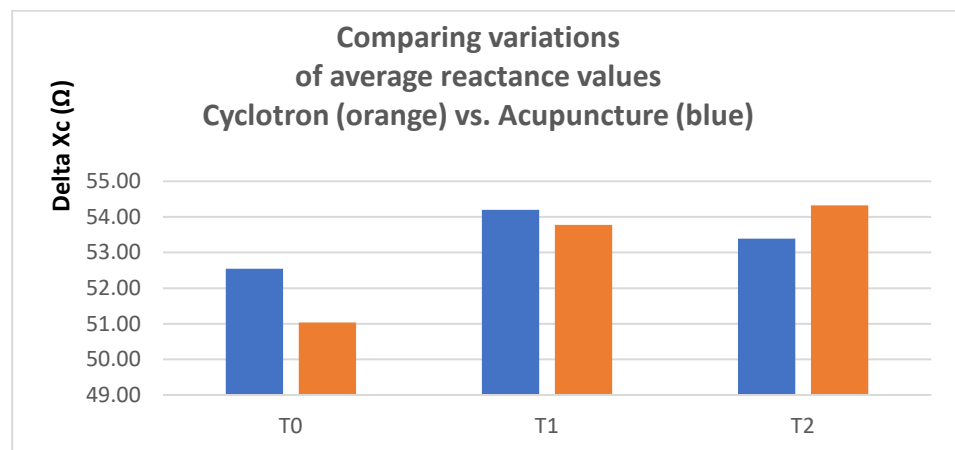


Figure 9. Average reactance increases more at T1 and less at T2, after acupuncture, and increases more after exposure to ion cyclotron emission, at the same acupuncture points.

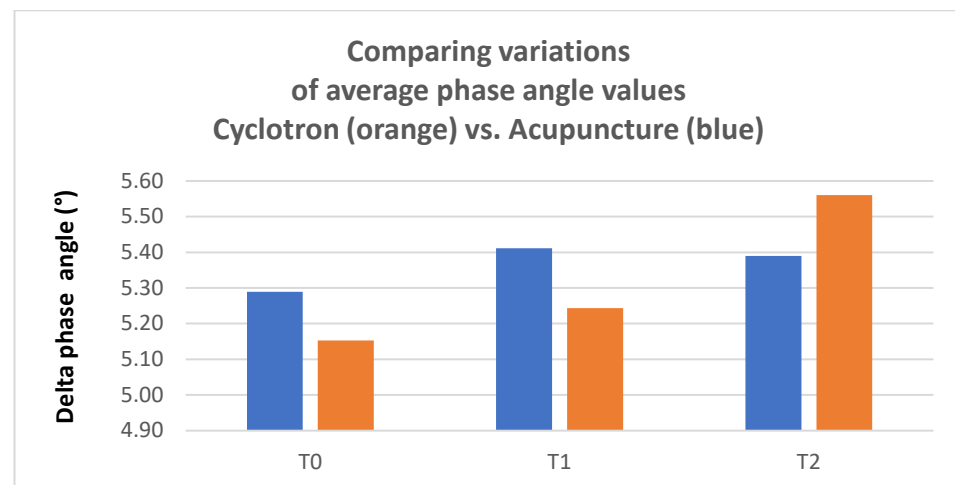


Figure 10. Average phase angle increases at T1 and increases further at T2 after exposure to ion cyclotron emission, while it increases at T1 and decreases at T2 after acupuncture at the same acupuncture points. It increases more after exposure to ion cyclotron emission than after acupuncture.

In the following Table 8, we compare the deltas between average values of resistance, reactance and phase angle at T0 and T2 for each group of treatments, by means of ion cyclotron exposures end acupuncture.

Table 8. Cyclotron vs. acupuncture—comparison of deltas of the T0 and T2 average values of resistance, reactance, and phase angle.

Cyclotronic	Acupuncture
T0–T2 resistance –13.2	T0–T2 resistance –2.2
T0–T2 reactance +3.3	T0–T2 reactance +0.8
T0–T2 phase angle +0.4	T0–T2 phase angle +0.1

The comparison of cyclotron vs. acupuncture shows that the cyclotron variations of the three parameters (resistance, reactance, and phase angle) at T2 are higher, indicating a greater effect of cyclotron treatment, albeit within the limits of the limited size of the sample. The T-test, in Table 9., shows that the variations are statistically meaningful.

Table 9. T test significance values for cyclotron vs. acupuncture at T2.

T Test Resistance Comparison at T2	$p = 0.0062$	$p < 0.05$
T test reactance comparison at T2	$p = 0.0001$	$p < 0.001$
T test phase angle comparison at T2	$p = 1.581 \times 10^{-5}$	$p < 0.0001$

5. Theoretical Background: Role of the Nonlinear Dynamics of Self-Organization in Alive

As expected from the consolidated theory on the function of acupuncture, after acupuncture on acupoints with proved effect, 8 h later, the electrical resistance decreases while the reactance and phase angle increase. This is in accordance with what happens when the amount of intracellular water is greater than extracellular water. The same happens even more markedly with exposure to the cyclotron frequencies.

The above results suggest the following explanation of the phenomenon: the intracellular water notoriously has greater conductivity and lower viscosity than ordinary bulk water, which justifies the decrease in resistance and the increase in inductive reactance by the treatment. The latter, in fact, opposes the passage of current and increases in relation to the increase in current. Once we consider the cell, in particular the cytoplasm, as an aqueous solution of ions and amino acids [23,24], the cyclotron frequency has the effect of producing ionic currents in cells. These results are compatible with the two-phase water model that arises from the quantum molecular physics of liquid water. According to this model, liquid water consists of a fraction of coherent water, where the water molecules are organized in clusters or coherent domains, which are formed by molecules whose quantum oscillations are in phase, and of an incoherent fraction, formed by molecules isolated unbound or linked by the weak hydrogen bonds. As indicated by this model, intracellular water has a greater fraction of coherence domains than extracellular water and the results of this experiment appear consistent with this hypothesis, indeed providing a therapy to increase intracellular water through acupuncture or exposure to cyclotron frequency.

The results reported here clearly indicate significant, experimentally measurable effects of the acupuncture treatment and cyclotron resonance exposure on electrical properties of acupuncture points and relation of these effects with the intra- and extracellular water in the nearby tissues. From a physical point of view, living matter is a highly nonlinear and anisotropic matter, which to a large extent can be compared to meso-phase liquid crystals with nonlinear electric and optical properties [5,29,30]. It is necessary to emphasize that, in general, in biological tissues and especially in the connective tissues, collagen fibers play a very important role. These fibers are quasi-one-dimensional macromolecules, which form liquid crystalline structures [31], whose electric and optical properties significantly depend on the amount and properties of water [32].

Along these elongated macromolecules made up of electric dipoles, water molecules align [33] and can oscillate in the direction parallel to macromolecules, forming a quasi-one-dimensional system. Thus, they form a coherent structure bound with the macromolecular chains, and form a new phase of water and coherence domains, able to trap and self-focus the electromagnetic field. Such coherence domains possess extra electrons, resulting in highly effective electron transport observed in aqueous systems. The existence of a charge separation between two aqueous phases, coherent and non-coherent, coexisting in water, has been experimentally demonstrated in [34,35], where it has been shown that an electric current flows in a conductor connecting two electrodes, one of which is placed in the interfacial water (called also as exclusion zone water, EZ-water), and the other in bulk (non-coherent) water.

The highly anisotropic properties of living tissues create conditions for energy, matter, and information flows which are non-uniformly distributed in the organism. It has been suggested in [5] that these flows of matter, energy, and information in such nonlinear systems can lead to the emergence of the dynamical order through self-trapping of the endogenous electromagnetic field in the form of the waveguides, which is dynamical and

not connected directly with the morphological structures. The flows of energy and self-trapped electromagnetic field along these dynamical pathways as waveguides can occur via soliton mechanism [5]. This can be compared with self-focusing of electromagnetic field in nonlinear media, for instance, in nonlinear optical crystals, in liquid crystals, etc., and its propagation in the form of solitons [36].

The complex pattern of such waveguides in the living matter is formed as the result of the interplay of (i) complex distribution of the electrical and optical properties and (ii) boundary conditions, including the shape of tissues, organs, and body. In view of such complex and dynamic geometry (partly because of bending role of joints), at some points, the waveguides approach the skin, where they form the nodes (again, this can be compared with the nodes as the connecting joints of the waveguides). Thus, it is quite natural that the electrical and optical properties of these nodes are very different from the nearby areas. Indeed, this has been confirmed experimentally [37–43] (see also references therein). In particular, it has been shown that acupuncture points have higher electric conductivity, increased conductance and capacitance, reduced impedance, and elevated electrical potential compared to adjacent non-acupuncture points. For instance, the refractive index in the acupuncture points varies from 1.36 to 1.40: in the range 1.41 to 1.49 in epidermal tissues and 1.36 to 1.41 in dermal tissues over the wavelength range [42,44]. This can be compared with the refractive index 1.373 (1.380 and 1.401) of the human cornea and 1.386–1.406 of the human lens [45], which are significantly higher than the refractive index of 1.33 for bulk water.

Moreover, it has been shown experimentally that there might be some changes in the electrical properties of acupuncture points and that these changes are correlated to certain clinical conditions. Moreover, investigations, reported in [46], have demonstrated that electrodermal measurements of acupuncture points may be used as a diagnostic tool for respiratory conditions. These conditions depend essentially on the efficiency of the charge transport in redox processes, in which the essential role belongs to solitons [47] (recall, solitons are special types of nonlinear localized solitary waves which can propagate in the system without energy dissipation). The elongated structures of water molecules surrounding macromolecules, such as collagen fibers, are connected by hydrogen bonds and form dynamical ice-like structures, which support the existence of solitons [48], whose dynamics can also be affected by external stimuli.

Solitons in the pathways can be stimulated either by intrinsic dynamics or by external stimuli, which, applied to the acupuncture points, can induce changes of the ratio intra- and extracellular water, induce changes in the interfacial water, and thus, affect the electrical and optical properties of the corresponding points: it has been shown that aqueous systems are very sensitive to ultra-weak external factors [49]. These changes can improve or even create conditions necessary for existence and launching of solitons, thus resulting in the enhancement of the efficiency of the corresponding channels.

It is also worth stressing that in our opinion, the finite variability of the acupuncture points positions indicates that they are dynamical entities formed in the self-organization of the living matter, which depend on its metabolism and physiological conditions, among other factors. This conclusion naturally follows from the theoretical model discussed here.

Since according to this model, the coherence domains are free energy sources, which allow the ionic currents to overcome the thermal noise caused by the Brownian motion of the bulk molecules [25], a higher coherent fraction of the cytoplasmic water means a greater chemical activity of the cell, greater trophism, greater cell tone, and ultimately, greater viability.

6. Conclusions

Both acupuncture and exposure to the alternating magnetic field, tuned with the geomagnetic field to generate ion-resonant cyclotron frequencies, result in a decrease in resistance and an increase in reactance and phase angle of impedance at the points of application. This effect leads to an increase of intracellular water, which in turn indicates

a greater level of coherence, a greater quantity of free energy, available for chemical activity, higher efficiency of charge transport processes, and thus, higher efficiency of the metabolism, and ultimately higher cell viability.

Indeed, the experimental results demonstrate not simply supplementary effects of weak external stimuli, but a qualitatively different effect, i.e., synergy, in particular, between ELF and acupuncture. This is another indication of the nonlinear character of the processes in living matter/biological systems.

Further research is needed to consolidate the results of this experiment as well as to highlight the opposite effect: induction of the efflux of intracellular water into the volume of extracellular water through the use of cyclotron resonance suitable to modulate the ion-gated membrane channels.

Author Contributions: Conceptualization, A.L., L.G. and L.B.; methodology, A.L., S.L., L.S., S.B., F.P. and M.I.P.; software, M.P.; validation, A.L., M.I.P. and L.G.; formal analysis, A.L. and L.B.; investigation, A.L., L.G. and L.B.; resources, M.P., M.I.P. and L.G.; data curation, A.L., S.L., L.S., S.B., F.P. and M.P.; writing—original draft preparation, A.L.; writing—review and editing, L.G. and L.B.; visualization, A.L.; supervision, L.G.; project administration, A.L., S.L. and L.S.; funding acquisition, A.L., S.L. and L.S. All authors have read and agreed to the published version of the manuscript.

Funding: This research was funded as work in economics by the Paracelso Institute and by the Nationale Academy of Ukraine, thanks to the scientific project 01122U000887 with reference to the contribution of L.B.

Institutional Review Board Statement: The design, study methods, and the research informed consent form were reviewed by the Ethics Committee of the Interuniversity Commission for Research on Acupuncture, an organism composed of University Professors established by AIAM (Italian Association of Acupuncture-Moxibustion and Traditional Chinese Medicine) and its approval data is 20 July 2018.

Informed Consent Statement: Informed consent was obtained from all the subjects involved in the study.

Data Availability Statement: The data presented in this study are available on request from the Paracelso Institute due to privacy.

Acknowledgments: Many thanks to Enrico D’Emilia, whose knowledge and experience made setting up the ICR device possible. We acknowledge the scientific project 0122U000887 of the National Academy of Sciences of Ukraine. which made possible the contribution of L.B.

Conflicts of Interest: The authors declare no conflict of interest. The funders had no role in the design of the study; in the collection, analyses, or interpretation of data; in the writing of the manuscript; or in the decision to publish the results.

References

1. Reichmanis, M.; Marion, A.A.; Becker, R.O. D.C. Skin conductance variation at acupuncture loci. *Am. J. Chin. Med.* **1976**, *4*, 69–72. [[CrossRef](#)]
2. Shang, C. The past, present and future of meridian system research. *Clin. Acupunct. Orient. Med.* **2000**, *1*, 115–124. [[CrossRef](#)]
3. Wang, K.; Liu, J. Needling sensation receptor of an acupoint supplied by the median nerve—studies of their electrophysiological characteristics. *Am. J. Chin. Med.* **1985**, *46*, 2097–2103. [[CrossRef](#)]
4. Tiller, W.A. What do electrodermal diagnostic acupuncture instruments really measure. *Am. J. Acupunct.* **1987**, *15*, 18–23.
5. Brizhik, L.S.; Del Giudice, E.; Maric-Oehler, W.; Popp, F.A.; Schlebusch, K.P. On the dynamics of self-organization in living organisms. *Electromagn. Biol. Med.* **2009**, *28*, 28–40. [[CrossRef](#)]
6. Sitko, S.P. The Realization of Genoma in the notions of physics of the alive Quantum Informational Medicine. *QIM Belgrade Proc.* **2011**, *4*, 30–41.
7. Arani, R.; Bono, I.; Del Giudice, E.; Preparata, G. QED Coherence and Thermodynamics of water. *Int. J. Mod. Phys. B* **1995**, *9*, 1813–1841. [[CrossRef](#)]
8. Liboff, A.R. A human source for ELF magnetic perturbations. *Electromagn. Biol. Med.* **2016**, *35*, 337–342. [[CrossRef](#)]
9. De Ninno, A.; Pregnolato, M. Electromagnetic homeostasis and the role of low-amplitude electromagnetic fields on life organization. *Electromagn. Biol. Med.* **2017**, *36*, 115–122. [[CrossRef](#)]
10. D’Emilia, E.; Giuliani, L.; Lisi, A.; Ledda, M.; Grimaldi, S.; Montagnier, L.; Liboff, A.R. Lorentz force in water: Evidence that hydronium cyclotron resonance enhances polymorphism. *Electromagn. Biol. Med.* **2015**, *34*, 370–375. [[CrossRef](#)]

11. D'Emilia, E.; Ledda, M.; Foletti, A.; Lisi, A.; Giuliani, L.; Grimaldi, S.; Liboff, A.R. Weak-field H_3O^+ ion cyclotron resonance alters water refractive index. *Electromagn. Biol. Med.* **2017**, *36*, 55–62. [CrossRef] [PubMed]
12. Pan, L.J.; Zhang, X.Q.; Liu, J.; Li, T.Y.; Xu, Y.Y.; Song, X.D.; She, Y.F.; Zhang, J.C.; Fan, X.S.; Jia, C.S. Progress of researches on electrical characteristics of meridian and acupoints in recent 10 years. *Zhen Ci Yan Jiu Acupunct. Res.* **2020**, *45*, 77–82. [CrossRef]
13. Khorsand, A.; Zhu, J.; Bahrami-Taghanaki, H.; Baghani, S.; Ma, L.; Rezaei, S. Investigation of the electrical impedance of acupuncture points and non-acupuncture points, before and after acupuncture, using a four-electrode device. *Acupunct. Med.* **2015**, *33*, 230–236. [CrossRef] [PubMed]
14. Geesing, J.H.; Meijer, D.K.F. Bio-soliton model that predicts non-thermal electromagnetic frequency bands, that either stabilize or destabilize living cells. *Electromagn. Biol. Med.* **2017**, *36*, 357–378. [CrossRef] [PubMed]
15. Istituto Paracelso. *Consenso Informato*; Istituto Paracelso: Rome, Italy, 2021.
16. Selvaggio, G.; Pearlstein, R.A. Biodynamics: A novel quasi-first principles theory on the fundamental mechanism of cellular function/dysfunction and the pharmacological modulation thereof. *PLoS ONE* **2018**, *13*, e0202376. [CrossRef] [PubMed]
17. Castizo-Olier, J.; Iruetia, A.; Jemni, M.; Carrasco-Marginet, M.; Fernandez-Garcia, R.; Rodriguez, F.A. Bioelectrical impedance vector analysis (BIVA) in sport and exercise: Systematic review and future perspectives. *PLoS ONE* **2018**, *13*, e0197957. [CrossRef]
18. Buffa, R.; Saragat, B.; Cabras, S.; Rinaldi, A.C.; Marini, E. Accuracy of specific BIVA for the assessment of body composition in the United States population. *PLoS ONE* **2013**, *8*, e58533. [CrossRef]
19. Norman, K.; Stobäus, N.; Pirlich, M.; Bösby-Westphal, A. Bioelectrical phase angle and impedance vector analysis-clinical relevance and applicability of impedance parameters. *Clin. Nutr.* **2012**, *31*, 854–861. [CrossRef]
20. Carrasco-Marginet, M.; Castizo-Olier, J.; Rodríguez-Zamora, L.; Iglesias, X.; Rodríguez, F.A.; Chaverri, D.; Brotons, D.; Iruetia, A. Bioelectrical impedance vector analysis (BIVA) for measuring the hydration status of young elite synchronized swimmers. *PLoS ONE* **2017**, *12*, e0178819. [CrossRef]
21. Piccoli, A.; the Italian HD-BIA Study Group. Identification of operational clues to dry weight prescription in hemodialysis issuing bioimpedance vectoranalysis. *Kidney Int.* **1998**, *53*, 1036–1043. [CrossRef]
22. Edefonti, A.; Loi, S.; Ardissino, G.; Dagnino, L.; Ghio, L.; Damiani, B.; Sandoval Diaz, M. Use of bioimpedance (BIA) to modify dry weight in patients on chronic hemodialysis (HD). *J. Am. Soc. Nephrol.* **1998**, *9*, 247A.
23. Ronco, C.; McCullough, P.; Anker, S.D.; Anand, I.; Aspromonte, N.; Bagshaw, S.M.; Bellomo, R.; Berl, T.; Bobek, I.; Cruz, D.N.; et al. Cardio-renal syndromes: Report from the consensus conference of the acute dialysis quality initiative. *Eur. Heart J.* **2010**, *31*, 703–711. [CrossRef] [PubMed]
24. Di Somma, S.; Lukaski, H.C.; Codognotto, M.; Peacock, W.F.; Fiorini, F.; Aspromonte, N.; Ronco, C.; Santarelli, S.; Lalle, I.; Autunno, A.; et al. Consensus paper on the use of BIVA. *Emerg. Care J.* **2011**, *7*, 6–14. [CrossRef]
25. Zhadin, M.N.; Novikov, V.V.; Barnes, F.S.; Pergola, N.F. Combined action of static and alternating magnetic fields on ionic current in aqueous glutamic acid solution. *Bioelectromagnetics* **1998**, *6*, 41–45. [CrossRef]
26. Giuliani, L.; Grimaldi, S.; Lisi, A.; D'Emilia, E.; Bobkova, N.; Zhadin, M. Action of combined magnetic fields on aqueous solution of glutamic acid: The further development of investigations. *Biomagn. Res. Technol.* **2008**, *6*, 1. [CrossRef]
27. Del Giudice, E.; Giuliani, L. Coherence in Water and the kT Problem in Living Matter. Non-Thermal Effects and Mechanisms of Interaction between Electromagnetic Fields and Matter. *Eur. J. Oncol.* **2010**, *5*, 7–23. Available online: http://www.teslabel.be/PDF/ICEMS_Monograph_2010.pdf (accessed on 8 June 2022).
28. Haagenen, J.A.J.; Bache, M.; Giuliani, L.; Blom, N.S. Effects of resonant electromagnetic fields on biofilm formation in *Pseudomonas aeruginosa*. *Appl. Sci.* **2021**, *11*, 7760. [CrossRef]
29. Kreis, R.; Boesch, C. Liquid crystal-like structure of human muscle demonstrated by in vivo observation of direct dipolar coupling of in localized proton magnetic resonance spectroscopy. *J. Magn. Res. B* **1994**, *104*, 189–192. [CrossRef]
30. Ho, M.W.; Zhou, Y.M.; Haffagee, J.; Watton, A.; Musumeci, F.; Privitera, G.; Scordino, A.; Triglia, A. The liquid crystalline organism and biological water. In *Water in Cell Biology*; Springer: Dordrecht, The Netherlands, 2006; pp. 1–16. [CrossRef]
31. Ho, M.-W.; Knight, D.P. The acupuncture system and the liquid crystalline collagen fiber of the connective tissues. *Am. J. Clin. Med.* **2001**, *26*, 251–263. [CrossRef]
32. Scordino, A.; Grasso, R.; Gulino, M.; Lanzano, L.; Musumeci, F.; Privitera, G.; Tedesco, M.; Triglia, A.; Brizhik, L. Delayed luminescence from collagen as arising from soliton and small polaron states. *Int. J. Quant. Chem.* **2010**, *110*, 221–229. [CrossRef]
33. Del Giudice, E.; De Ninno, A.; Fleischmann, M.; Mengoli, G.; Milani, M.; Talpo, G.; Vitiello, G. Coherent quantum electrodynamics in living matter. *Electromagn. Biol. Med.* **2005**, *24*, 199–210. [CrossRef]
34. Del Giudice, E.; Fleischmann, M.; Preparata, G.; Talpo, G. On the 'unreasonable' effect of ELF magnetic fields upon a system of ions. *Bioelectromagnetics* **2002**, *23*, 522–530. [CrossRef] [PubMed]
35. Zhadin, M.; Giuliani, L. Some Problems of Modern Bioelectromagnetics. *Electrom. Biol. Med.* **2006**, *25*, 227–243. [CrossRef]
36. Zakharov, V.E.; Shabat, A.B. Exact theory of two-dimensional self-focusing and automodulation of waves in nonlinear media. *Sov. J. Exp. Phys.* **1971**, *61*, 118–134.
37. Niboyet, J.E.H. Part 2: Lower electrical resistance on skin surface corresponding to cutaneous acupuncture points and meridians. In *Treatise on Acupuncture*; Niboyet, J.E.H., Bourdiol, R.J., Regard, P.G., Eds.; Maisonneuve: Paris, France, 1963; pp. 326–333. (In French)
38. Thong, T.; Colbert, A. Correlating heart rate variability with skin impedance measurements. *Conf. Proc. IEEE Eng. Med. Biol. Soc.* **2005**, *5*, 4947–4950. [CrossRef]

39. Ahn, A.C.; Colbert, A.P.; Anderson, B.J.; Martinsen, Ø.G.; Hammerschlag, R.; Cina, S.; Wayne, P.M.; Langevin, H.M. Electrical Properties of Acupuncture Points and Meridians: A Systematic Review. *Bioelectromagnetics* **2008**, *29*, 245–256. [[CrossRef](#)] [[PubMed](#)]
40. Wei, J.; Mao, H.; Zhou, Y.; Wang, L.; Liu, S.; Shen, X. Research on Nonlinear Feature of Electrical Resistance of Acupuncture Points. *Evid. Based Complement. Altern. Med.* **2012**, *2012*, 179657. [[CrossRef](#)]
41. Khlopets'kaLarysa, I.; HorkovenkoNataliya, L.; Zukow, W. Electrical conductivity of some points of acupuncture correlates with age, blood pressure and heart rate variability. *J. Educ. Health Sport* **2017**, *7*, 94–103, eISSN 2391-8306.
42. Zhao, N.; Lin, Q.; Yao, K.; Zhang, F.; Tian, B.; Chen, F.; Jiang, Z. Simultaneous Measurement of Temperature and Refractive Index Using High Temperature Resistant Pure Quartz Grating Based on Femtosecond Laser and HF Etching. *Materials* **2021**, *14*, 1028. [[CrossRef](#)]
43. Gafarov, G.A. Acupuncture research methods. *J. Appl. Biotechnol. Bioeng.* **2020**, *7*, 276–278. [[CrossRef](#)]
44. Lister, T.; Wright, P.A.; Chappell, P.H. Optical properties of human skin. *J. Biomed. Opt.* **2012**, *17*, 090901. [[CrossRef](#)] [[PubMed](#)]
45. Patel, S.; Marshall, J.; Fitzke, F.W., 3rd. Refractive index of the human corneal epithelium and stroma. *J. Refract. Surg.* **1995**, *11*, 100–105. [[CrossRef](#)]
46. Hong, H. Electrodermal Measurement of Acupuncture Points May Be a Diagnostic Tool for Respiratory Conditions: A Retrospective Chart Review. *Med. Acupunct.* **2016**, *28*, 138–148. [[CrossRef](#)]
47. Brizhik, L. Influence of electromagnetic field on soliton mediated charge transport in biological systems. *Electromagn. Biol. Med.* **2015**, *34*, 123–132. [[CrossRef](#)] [[PubMed](#)]
48. Antonchenko, V.Y.; Davydov, A.S.; Zolotaryuk, A.V. Solitons and proton motion in ice-like structures. *Phys. Status Solidi B* **1983**, *115*, 945–952. [[CrossRef](#)]
49. Brizhik, L.S.; Del Giudice, E.; Tedeschi, A.; Voeikov, V.L. The role of water in the information exchange between the components of an ecosystem. *Ecol. Model.* **2011**, *222*, 2869–2877. [[CrossRef](#)]